Nanoscale Advances

ROYAL SOCIETY OF CHEMISTRY

PAPER

View Article Online
View Journal | View Issue

Check for updates

Cite this: *Nanoscale Adv.*, 2024, **6**, 6328

Freon–CO_2-assisted purification of single-walled carbon nanotubes†

Yiman Huang,[a] Xiao Zhu,*[a] Tao Chen,[b] Hongyan Li,[b] Liang Han[c] and Xilai Jia *[c]

Received 24th July 2024
Accepted 8th September 2024

DOI: 10.1039/d4na00610k

rsc.li/nanoscale-advances

With the rapidly growing applications, efficient purification of single-walled carbon nanotubes (SWCNTs) has become one of the key problems. This paper proposes Freon–CO_2-assisted purification of SWCNTs, where CO_2 can oxidize the graphitized carbon layer to expose iron (Fe) impurities, while the chlorine from Freon can react with the Fe impurities to form low-boiling-point metal chlorides that can be eliminated in a gas stream. After an acid washing with a very small amount of hydrochloric acid, the last remaining metal impurities are removed and highly pure SWCNTs are produced. Compared with traditional strong-acid-oxidation purification or high-temperature-vacuum purification, this method can maintain the structure and length of the SWCNTs. Raman spectra show that an I_G/I_D ratio of more than 100 can be obtained. This purification method can maintain the microstructure and excellent properties of SWCNTs and provide a solution for the preparation of high-quality SWCNTs to exert their properties.

1 introduction

Single-walled carbon nanotubes (SWCNTs) have unique physicochemical properties such as high mechanical strength,[1] high electrical conductivity,[2] and good stability, making them wildly used in the field of materials science.[3] Their applications have witnessed rapid growth in electric vehicles, polymer nanocomposites, and others.[4] Now, they have been successfully used in energy storage as conductive additives in lithium-ion batteries (LIBs) and have shown better performance than traditional carbon black.[5] When using CNTs in LIBs, one of the critical problems we have to solve is the removal of metal impurities,[6–9] which is attributed to the iron-based catalyst used in the production process of carbon nanotubes by the Chemical Vapor Deposition (CVD) method.[10–12] Metal impurities will result in self-discharge and decrease the lithium-ion battery performance, and more seriously, cause some safety problems after repeated charge/discharge cycles.[13,14] Therefore, the purity of SWCNTs is important and it has critically limited their high-end applications in energy storage.[15]

To date, several kinds of multiwalled carbon nanotubes (MWCNTs) have achieved large-scale production and been used in various energy-storage applications. Typically, aggregated MWCNTs and aligned MWCNTs have been produced on a large scale and used for commercial LIBs.[16–18] Compared with aggregated MWCNT powders, aligned MWCNTs consist of nanotubes growing in one direction and show weaker interactions. This makes aligned MWCNTs much easier to disperse in manufacturing and show an increasing trend in applications.[19,20] The purification of these two kinds of MWCNTs is usually done by simple acid washing or high temperature vacuum purification. However, these two traditional methods are not suitable for the purification of SWCNTs.

As we know, the impurities of CNTs mainly include amorphous carbons, onion-like carbons, and resultant metals that come from the catalyst.[21] It has been found that the reaction energies of amorphous carbons, onion-like carbons,[22–24] and crystalline CNTs are different,[25] where amorphous carbons can be burned by precise control of oxidation temperature in air or oxygen. As for the metal impurities, the common removal method was acid washing using HCl, HNO_3, HF, H_2SO_4, or their mixture.[26–29] Most metal impurities can be washed away; for example, the Fe impurity of double-walled carbon nanotubes (DWCNTs) can be reduced to less than 1000 ppm after times of acid washing of pre-oxidized DWCNTs.[30] However, washing can hardly reduce Fe impurities to a lower degree even after several times of acid washing.[31–36] Besides, the huge use of acid washing causes severe environmental pollution. This great challenge has limited the decrease of the cost of CNTs in battery applications and other developments.

The main reasons for the ineffective purification of metals through acid washing are that the metals are confined in an internal nanotube or the ions are encapsulated in onion carbons by graphitic layers.[37] Even though the pre-oxidation treatment can open most coated ions in onion carbons, the Fe particles coated by graphitic layers have difficulty accessing the

[a]College of Science, China Agricultural University, Beijing 100091, P. R. China. E-mail: zhuxiao@cau.edu.cn
[b]State Grid Jilin Electric Power Research Institute, Changchun, 130021, P. R. China
[c]School of Materials Science and Engineering, University of Science and Technology Beijing, Beijing 100083, P. R. China. E-mail: jiaxl@ustb.edu.cn

† Electronic supplementary information (ESI) available. See DOI: https://doi.org/10.1039/d4na00610k

acid due to the hydrophobicity of the graphitic layers, thereby making the metals difficult to remove by acid washing.

In this context, a high-temperature treatment that has been used in the purification of natural graphite has been proposed for the purification of CNTs in the past few years.[38] It has been reported that high-temperature purification of DWCNTs can remove almost all the metal impurities;[39] however, it is found that DWCNTs can be joined together and become MWCNTs when the temperature is higher than 1700 °C.[40] As for MWCNTs, they can bear higher temperatures. Prof. Wei's previous results show that 99.99% purity of MWCNTs can be obtained after 2200 °C treatment.[39] Due to the samples available, the CNTs used in the past are almost aggregated or aligned MWCNT powders. Today, with better properties and decreased cost, the use of SWCNTs has greatly boosted; however, their purification methods are almost blank, which has become a key step in SWCNT application.

It was found that iron chloride is easy to sublimate, and its theoretical sublimation temperature is low.[26–28] Thereby, the Fe impurities can be oxidized by chlorine to generate $FeCl_3$, and then $FeCl_3$ can be gasified and separated from SWCNTs by heating, achieving the purpose of purifying SWCNTs. Compared with Freon, the direct use of Cl_2 can also purify SWCNTs. However, Cl_2 has strong oxidizing properties and can cause serious corrosion to the equipment. The selection of Freon is more reasonable. Since chlorine is provided by the decomposition of Freon, we name this purification process "Freon–CO_2-assisted purification". Fig. 1 shows the schematic of the Freon–CO_2-assisted purification process. First, the SWCNT sample is pre-oxidated in air flow at 400 °C, in which iron metal residues are oxidized into iron oxides and amorphous carbon is burned off. Then, the introduced CO_2, as well as the generated CO_2 in the purification process, will react with the graphitic carbon layer coated on iron metal nanoparticles at a higher temperature (800 °C), followed by the reaction between iron oxides and Cl_2 generated from the decomposition of Freon. Finally, the remaining iron metal impurities will be further removed by acid washing with HCl solution. Compared with high-temperature treatment, the Freon–CO_2-assisted purification can not only greatly reduce energy consumption, but also maximize maintainance of the structural integrity of the SWCNTs and reduce the occurrence of coalescence. This paper will focus on systematically studying the process and mechanism of purifying SWCNTs based on the Freon–CO_2-assisted purification method, hoping to solve the critical problem between preparation and battery applications of SWCNTs and promoting the high-end application of SWCNTs.

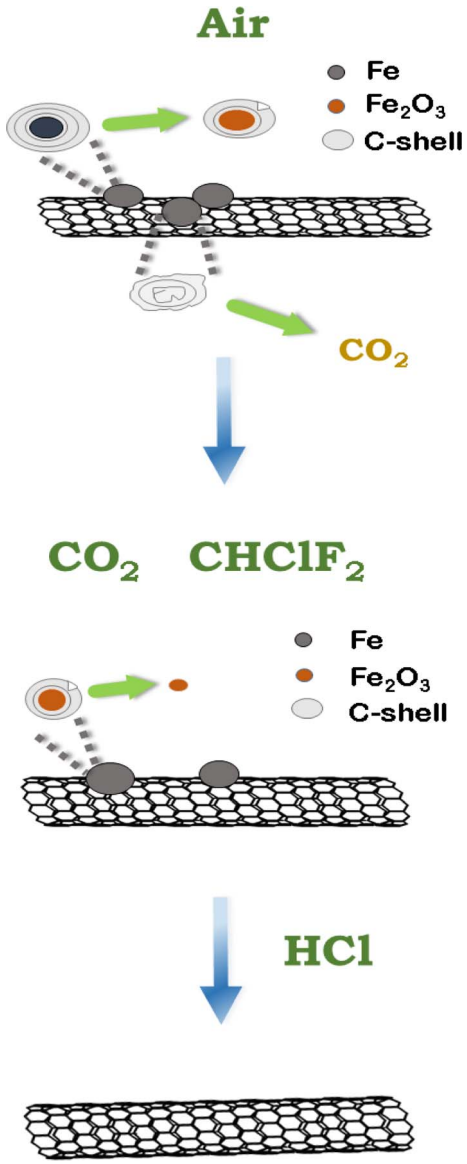

Fig. 1 Schematic of the Freon–CO_2-assisted purification process of SWCNTs.

2 Methods

2.1 Air pre-oxidation

Raw SWCNTs were provided by OCSiAl and were prepared by a unique CVD method. The air pre-oxidation process is detailed as: 0.2 g of the SWCNTs was added into a quartz boat, and the quartz boat was placed into a tube furnace. Then the furnace was heated to 400 °C at a rate of 10 °C min^{-1} under an argon flow of 200 mL min^{-1}. Subsequently, air was introduced into the furnace at 50 mL min^{-1} at a reaction time of 1 h. After that, air was turned off; the furnace was heated to 450 °C at a rate of 10 °C min^{-1} under an argon flow of 200 mL min^{-1} and maintained for 0.5 h.

2.2 Freon–CO_2-assisted purification and pickling

Following the pre-oxidation process, the furnace was heated to 800 °C at a rate of 10 °C min^{-1} under an argon flow of 200 mL min^{-1}, and then CO_2 and Freon were introduced into the furnace at 200 mL min^{-1} and 50 mL min^{-1}, respectively. The reaction time was 1 h. After that, CO_2 and Freon were turned off, and then the furnace was cooled down to room temperature under an argon flow of 200 mL min^{-1}. The obtained products were stirred in HCl aqueous solution at 60 °C for 48 h to remove the remaining metal catalyst impurities. In this process, two kinds of concentrations of HCl solution were used, that is,

0.01 mol L^{-1} and 6 mol L^{-1}, respectively. The as-obtained products were filtered, washed, and dried in a vacuum oven at 60 °C for 12 h. For the 0.01 mol L^{-1} HCl concentration, the as-obtained products were labeled as CF. As for the 6 mol L^{-1}HCl concentration, the as-obtained products were labeled as CF-1.

For comparison, the raw sample provided by OCSIAL without any treatment was labeled as RS. RS was pre-oxidized in air and then acid pickled with 6 mol L^{-1} HCl at 60 °C for 48 h to obtain the acid-washed sample, which was denoted as AS. RS was pre-oxidized in air, purified with the treatment of CO_2 at 800 °C for 1 h, and then acid pickled with 6 mol L^{-1} HCl at 60 °C for 48 h to obtain the CO_2-assisted purified sample, and this sample was denoted as CS. CS was further purified with the treatment of Freon at 800 °C for 1 h to obtain CF-2.

Similarly, the original sample of multi-walled carbon nanotubes without any treatment was labeled as RS-M. RS-M with the same treatment as that of CF and CF-1 were labeled as CF-M and CF-M1, respectively.

All the samples' purification details are summarized and listed in ESI Table S1.†

2.3 Characterization

Transmission electron microscopy (TEM) was conducted using a JOEL2010 at 120 kV to observe the microstructural changes of SWCNTs before and after purification. Thermogravimetric-differential thermal analysis (TGA) with air flow at a heating rate of 10 °C min^{-1} was used to determine the total carbon and metal content. Raman spectroscopy was used to analyze the structure of SWCNTs before and after purification. Raman spectra were recorded on a Renishaw (RW2000) with a wavelength of 532 nm and a 40 μm spot. XRD diffraction was used to observe the degree of graphitization of SWCNTs before and after purification. An X-ray diffractometer (DMAX-RB) uses copper as the target element for generating X-rays with a characteristic X-ray wavelength of $\lambda = 1.54184$ Å, a diffraction angle of 10 to 90° (2θ) and a scanning speed of 8° min^{-1}.

3 Results and discussion

3.1 Exploration of the reaction mechanism

The feasibility of the reaction of transition metal (mostly Fe, Co, and Ni) catalysts grown on SWCNTs was verified by comparison of the melting and boiling points of metal chlorides and their oxides. Fig. 2a shows that the boiling points of metal chlorides are usually much lower than the melting points of the metals and their oxides, especially the Fe catalyst. This gives opportunity for lower-temperature purification of the SWCNTs, which may bring on reduced energy consumption and circumvent the structural coalescence of the SWCNTs in traditional high-temperature vacuum purification.

Moreover, the high-boiling metal can be converted into a low-boiling chloride through the corresponding oxides. Taking the Fe catalyst used for the SWCNT growth of the OCSiAl sample as an example, we can first oxidize the Fe metal in air to form Fe_2O_3, and then Fe_2O_3 can react with chlorine to generate metal chloride vapor with a lower boiling point (Reaction 4). This reaction mechanism can be verified based on Gibbs free energy change calculations, as shown in Fig. 2b. The Gibbs free energy change for a certain chemical reaction was calculated from the standard Gibbs free energy of the substance: $\Delta_r G^{\theta}(T) = \sum_B \nu_B \Delta_f G_m^{\theta}(T)$. In the Freon–$CO_2$-assisted purification process of SWCNTs, the related reactions were

$$2CHClF_2\ (g) = C_2F_4\ (g) + 2HCl\ (g)\ (600\text{–}800\ ^\circ C)\ (\text{Reaction 1}) \quad (1)$$

$$2HCl\ (g) = H_2\ (g) + Cl_2\ (g)\ (\text{Reaction 2}) \quad (2)$$

$$C_2F_4\ (g) = 2C\ (s) + 2F_2\ (g)\ (\text{Reaction 3}) \quad (3)$$

$$4Cl_2\ (g) + 3C\ (s) + 2Fe_2O_3\ (s) = 4FeCl_2\ (g) + 3CO_2\ (g)\ (\text{Reaction 4}) \quad (4)$$

The Gibbs free energy change values of the reactions related to Fe impurities in the purification were calculated at different temperatures, and a linear fit was performed, as shown in Fig. 2b. Based on thermodynamic data from ref. 41, the standard Gibbs free energy change for Reaction 4 was less than zero

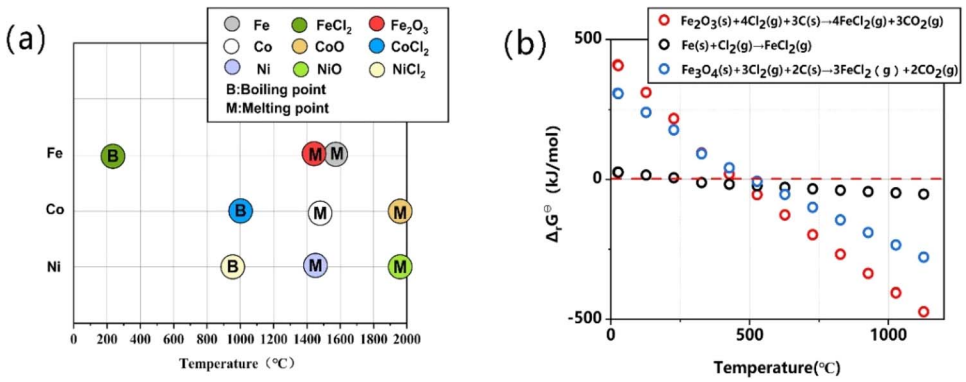

Fig. 2 (a) Melting and boiling points of substances related to the elements Fe, Co, and Ni. (b) Standard Gibbs free energy changes for reactions associated with Fe in purification processes of the SWCNTs.

for $T > 470$ °C. Moreover, this shows that the Fe nanoparticles are more preferable to be converted into $FeCl_2$ through the oxidized Fe_2O_3. The standard Gibbs free energies for $FeCl_2$, CO_2, and Fe_2O_3 were obtained by referring to the thermodynamic data, and the values of Cl_2 and C were zero.

Similarly, based on the calculation, $FeCl_3$ can also be produced. The reaction can be expressed as

$$6Cl_2\ (g) + 3C\ (s) + 2Fe_2O_3\ (s) = 4FeCl_3\ (g) + 3CO_2\ (g) \quad \text{(Reaction 5)} \tag{5}$$

Based on the theoretical prediction above, we put forward the "Freon–CO_2-assisted purification" technology. Fig. 3a provides the detailed experimental procedure to show the purification process. First, raw SWCNTs are pre-oxidated at 400 °C in an air flow, in which the Fe impurities are oxidized into iron oxides (*e.g.* Fe_2O_3) and amorphous carbon is burned off at the same time (as illustrated in Fig. 3b). This can increase the purity of SWCNTs and facilitates the subsequent Freon–CO_2-assisted purification process. Then, when heated to a higher temperature of *ca.* 800 °C, the introduced CO_2 will react with the graphitic carbon layer coated on the Fe impurities. Meanwhile, the introduced Freon will decompose to produce Cl_2, which will react with the exposed Fe and Fe_2O_3 impurities (as illustrated in Fig. 3d). Note that the air pre-oxidation produces moisture condensed at the end of the tube furnace (Fig. 3c). When Freon and CO_2 are introduced, the condensed moisture becomes green liquid at the end of the furnace (Fig. 3e), indicating the generation of ferrous chloride during the purification process. More importantly, this indicates that the Fe impurities can be eliminated in the gas stream and this will greatly reduce further acid consumption. Fig. 3f displays the fresh green liquid collected into the bottle after purification. After being placed in air for 48 h, it will be changed to yellowish-green in color (Fig. 3g), indicating the oxidation of ferrous ions

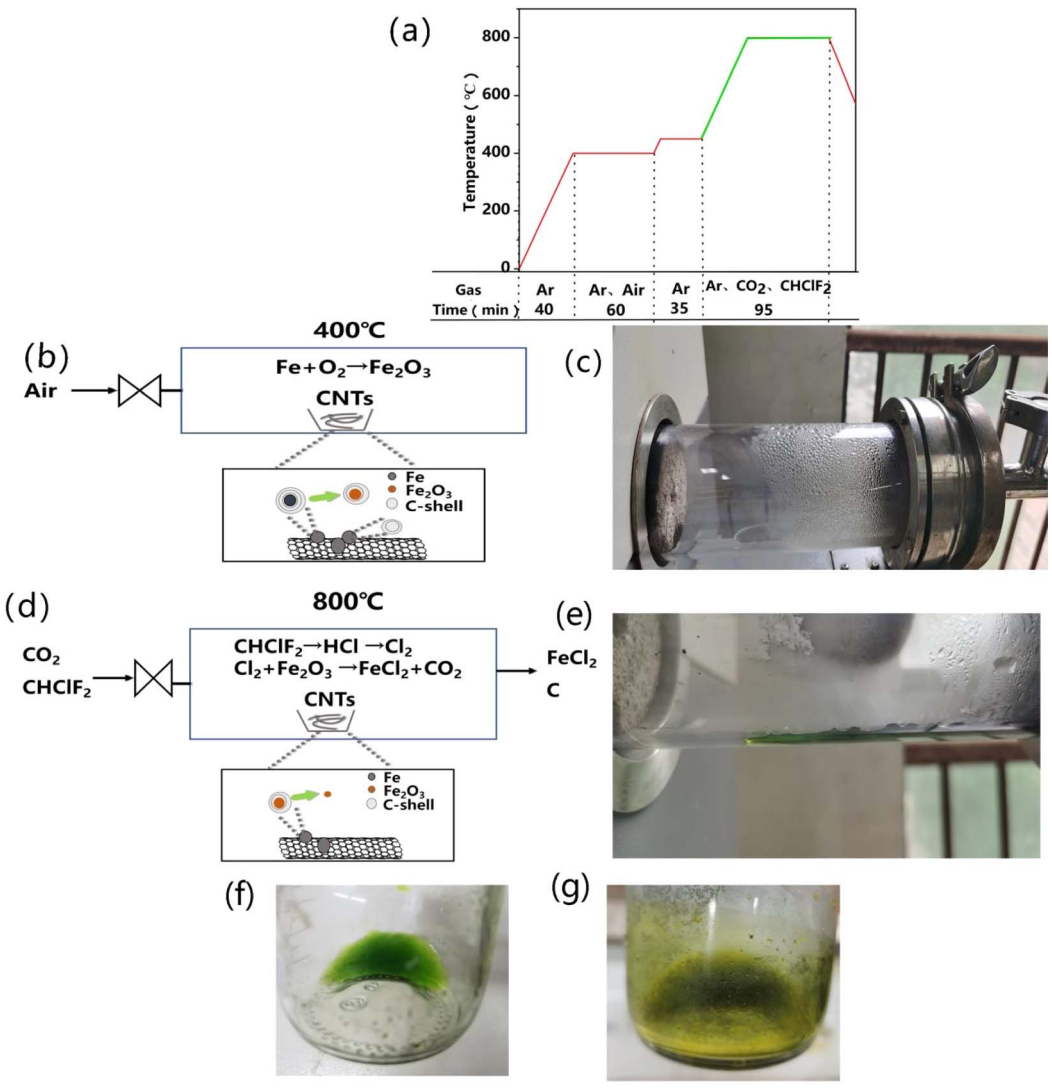

Fig. 3 (a) Diagram of the Freon–CO_2-assisted purification process. (b) Schematic of air pre-oxidation. (c) Moisture condensed at the end of the tube furnace. (d) Schematic of the Freon–CO_2-assisted purification process. (e) Liquid $FeCl_2$ at the end of the tube furnace. (f) Fresh liquid collected after the purification, and (g) liquid stayed in air for 48 h.

to iron ions. These results are consistent with the proposed reactions in the Freon–CO_2-assisted purification process. Moreover, the "Freon–CO_2-assisted purification" method is used mostly for Fe-catalyzed SWCNTs; as for Ni and Co, it has limitations since their chlorides is nearly 1000 °C.

3.2 Purification of SWCNTs

TEM images of the raw SWCNTs (RS, Fig. 4a and b) and purified SWCNTs (CF, Fig. 4c and d) were compared. Fig. 4a shows that black clusters of Fe nanoparticles are entangled with SWCNTs. The particle sizes are several nanometers. The graphite layer coated outside can be seen clearly in the magnified view (Fig. 4b), while, after Freon–CO_2-assisted purification, it is difficult to observe the Fe metal nanoparticles (Fig. 4c and d), which confirms that Freon–CO_2-assisted purification could effectively remove the iron catalyst nanoparticles, leaving the pure SWCNTs.

By comparing CS and CF in Table 1, it can be seen that the introduction of Freon in the purification process increases the purity from 98.0 wt% to 98.4 wt%. By comparing CF and CF-1 at the same time, it can be seen that the purity changes very little, which means that purity cannot be greatly improved by increasing the amount of acid, so the consumption of acid can be significantly reduced, subsequently reducing the waste liquid disposal. Compared to CF-1 which was purified by introducing CO_2 and Freon at the same time, the purity of CF-2 reaches 99.0 wt%, proving that the purification efficiency is obviously improved when CO_2 and Freon act on the sample successively.

Table 1 Purity and Raman I_G/I_D before and after purification of the SWCNT samples

Sample	Purity[a] (%)	I_G/I_D[b]
RS	85.8	27.9
AS	97.0	29.5
CS	98.0	30.2
CF	98.4	44.2
CF-1	98.6	45.6
CF-2	99.0	103.5

[a] The initial mass of the sample minus its ash mass after one hour of treatment at 800 °C in an air atmosphere and then divided by the initial mass. [b] The intensity ratio of the G-band to the D-band.

The Raman spectra of both RS and CF show characteristic peaks of SWCNTs, with strong G peaks and weak D peaks at 1590 cm^{-1} and 1350 cm^{-1}, respectively, indicating the high-

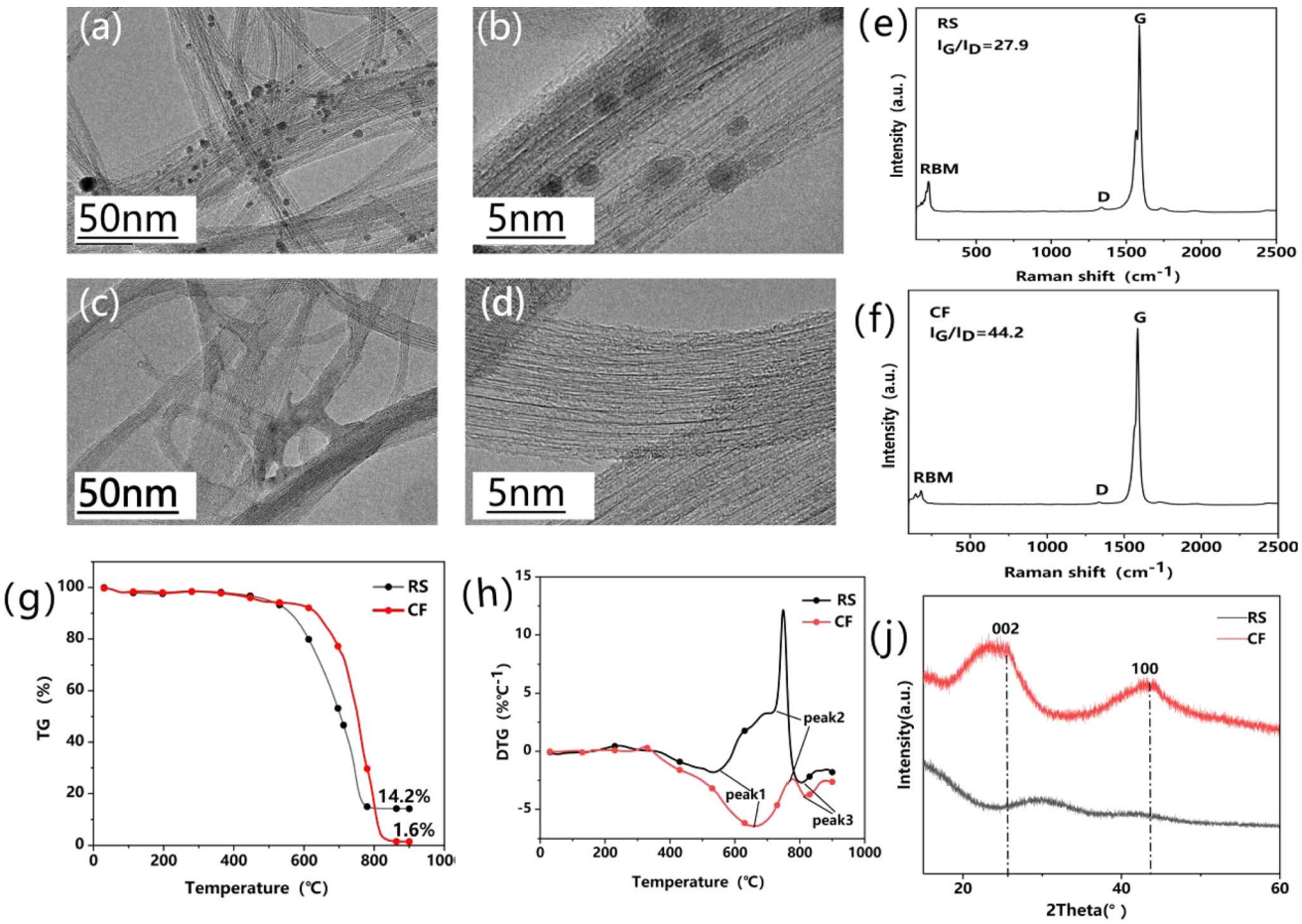

Fig. 4 TEM images of (a and b) RS and (c and d) CF. Raman spectra of (e) RS and (f) CF. (g) TGA and (h) DTG curves of RS and CF. (i) XRD patterns of RS and CF.

quality of SWCNTs. Compared to RS, the intensity ratio of the G-band to the D-band (I_G/I_D) for CF increased from 27.9 to 44.2 (Fig. 4e and f), owing to the removal of iron metal nanoparticles and amorphous/defective carbon. In particular, the I_G/I_D value of CF-2 is as high as 103.5, which further indicates the enhanced purification efficiency. To the best of our knowledge, an I_G/I_D ratio of more than 100 has rarely been obtained in SWCNT purification,[42,43] which supports that the proposed "Freon–CO_2-assisted purification" technology can produce high-quality SWCNTs.

The mass percentage of RS and CF was determined by thermogravimetric analysis (Fig. 4g). Compared to RS with a 14.2 percentage of the weight left above 800 °C, only 1.6 wt% was left for CF, further indicating the removal of iron metal nanoparticles. To further verify the purification efficiency, the DTG curves were fitted (Fig. 4h). This shows that the positions of the three combustion peaks of CF are shifted to the high-temperature range, which indicates that the purity of the CF sample is improved. Fig. 4i shows the XRD patterns of RS and CF. It can be observed that CF exhibits typical diffraction peaks of graphite at 25.8° and 43.2°, corresponding to (002) and (100) crystallographic diffraction, which proves that CF is much more graphitized, with a substantial increase in the purity in comparison with RS.

3.3 Purification of arrayed MWCNTs

To illustrate the effectiveness of this method, vermiculite-arrayed MWCNTs were subjected to Freon–CO_2-assisted purification. TEM images of the pristine MWCNTs (RS-M, Fig. 5a and b) and purified MWCNTs (CF-M, Fig. 5c and d) were compared. Fig. 5a shows that a certain amount of metal nanoparticles is entangled with the MWCNTs with particle sizes of 20 nanometers from the enlarged observation in Fig. 5b. Similar to SWCNTs, the metal nanoparticles are also coated with graphitic layers. After the Freon–CO_2-assisted purification, the metal nanoparticles were hardly observed (Fig. 5c and d). These results support that the Freon–CO_2-assisted purification is effective in removing Fe catalyst nanoparticles. The Raman spectra of both RS-M and CF-M show the characteristic peaks of MWCNTs, in which the G-wave and D-wave peak segments are not separated (Fig. 5e and f). Compared to RS-M, the I_G/I_D value of CF-M increases from 0.64 to 0.78, indicating the enhanced graphitization and the quality of carbon nanotubes. Table 2 shows that the purity of CF-M1 (99.9 wt%) is just a little higher than that of CF-M (99.7 wt%) which was pickled with only

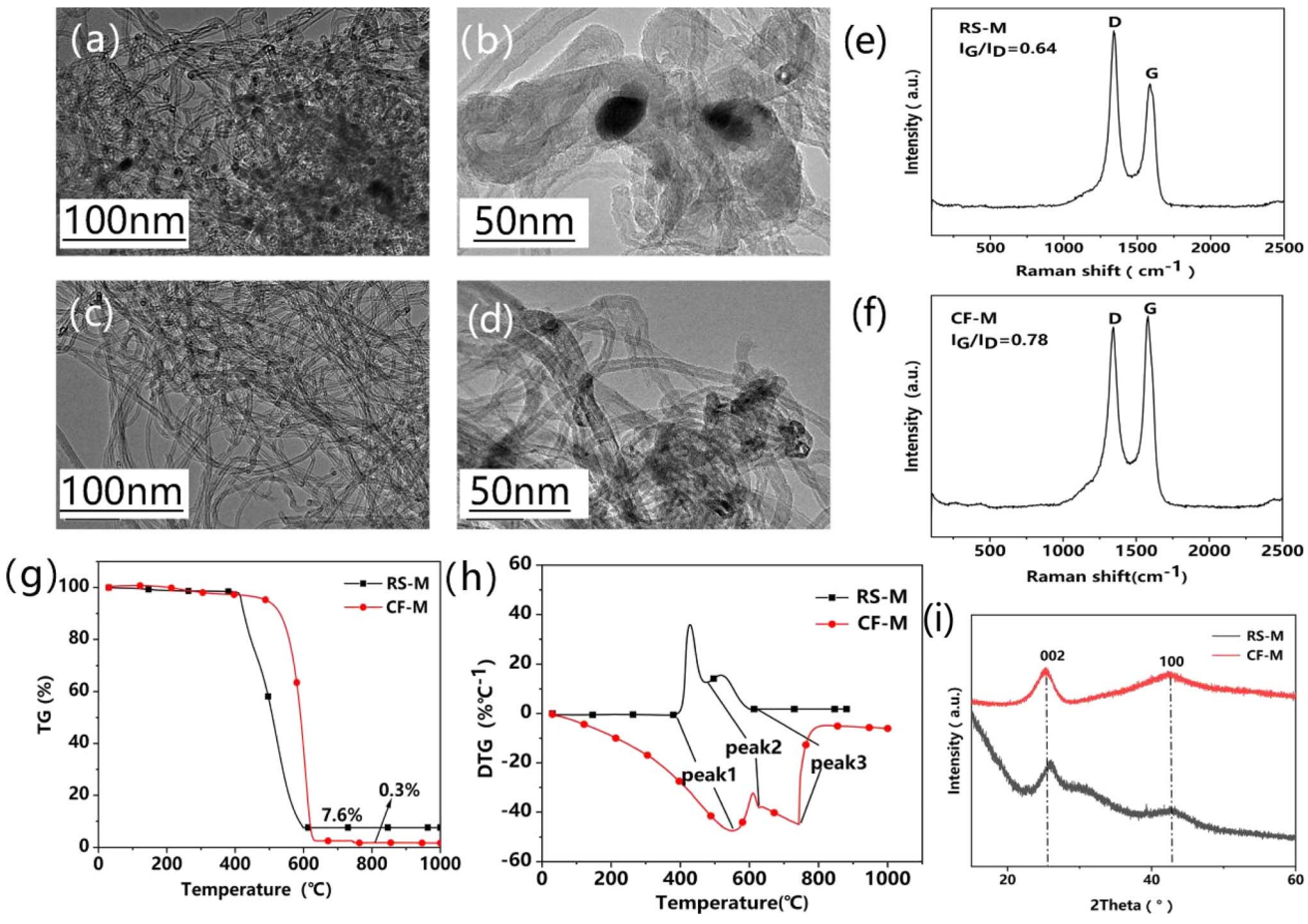

Fig. 5 TEM images of RS-M (a and b) and CF-M (c and d). Raman spectra of RS-M (e) and CF-M (f). (g) TGA curves of RS-M and CF-M. (h) DTG curves of RS-M and CF-M. (i) XRD patterns of RS-M and CF-M.

Table 2 Purity and Raman I_G/I_D before and after purification of the MWCNT samples

Sample	Purity[a] (%)	I_G/I_D[b]
RS-M	92.4	0.64
CF-M	99.7	0.78
CF-M1	99.9	0.83

[a] The initial mass of the sample minus its ash mass after one hour of treatment at 800 °C in an air atmosphere and then divided by the initial mass. [b] The intensity ratio of the G-band to the D-band.

0.01 mol L^{-1} HCl, further confirming the nonnecessity of high concentration pickling. A much lower weight is left for CF-M (0.3 wt%) in TG curves (Fig. 5g). The decomposition peak of CF-M moves to higher temperature in DTG curves (Fig. 5h), similar to the SWCNTs. All these verify the improved high purity of CF-M after purification. Compared to RS-M, the XRD pattern of CF-M exhibits enhanced diffraction peaks at (002) and (100) (Fig. 5i), indicating that the MWCNTs are more graphitized after purification.

4 Conclusions

In summary, "Freon–CO_2-assisted purification" technology has been proposed for purification of CNTs. This method is able to effectively purify SWCNTs and vermiculite-arrayed MWCNTs by removing residual metal nanoparticles and carbon impurities, leaving carbon tubes with an intact structure. The purity reaches 99.0 wt% for SWCNTs and 99.9 wt% for MWCNTs. During the purification process, pickling with only a very small amount of HCl can achieve the ideal purification effect, reducing the consumption of acid and waste disposal. This effective and low-energy consumption purification method will greatly promote the application of CNTs in high-end fields.

Data availability

The data supporting this article have been included as part of the ESI.†

Conflicts of interest

There are no conflicts to declare.

Acknowledgements

We thank professor Fei Wei of Tsinghua University for his support in electron microscope characterization. This work was supported by the science and technology research foundation of State Grid in 2022 (No. 5200-202229101A-1-1-ZN).

Notes and references

1 C. Luo, F. Li, D. Li, Q. Fu and C. Pan, Bioinspired Single-Walled Carbon Nanotubes as a Spider Silk Structure for Ultrahigh Mechanical Property, *ACS Appl. Mater. Interfaces*, 2016, **8**(45), 31256–31263.
2 M. Terrones, H. Terrones, M. S. Dresselhaus, G. Dresselhaus, J. C. Charlier and E. Hernández, Electronic, thermal and mechanical properties of carbon nanotubes, *Philos. Trans. R. Soc., A*, 2004, **362**(1823), 2065–2098.
3 R. Rao, C. L. Pint, A. E. Islam, R. S. Weatherup, S. Hofmann, E. R. Meshot, *et al.*, Carbon Nanotubes and Related Nanomaterials: Critical Advances and Challenges for Synthesis toward Mainstream Commercial Applications, *ACS Nano*, 2018, **12**(12), 11756–11784.
4 P. Zhai, J. A. Isaacs and M. J. Eckelman, Net energy benefits of carbon nanotube applications, *Appl. Energy*, 2016, **173**, 624–634.
5 W. Yuan, Y. Zhang, L. Cheng, H. Wu, L. Zheng and D. Zhao, The applications of carbon nanotubes and graphene in advanced rechargeable lithium batteries, *J. Mater. Chem. A*, 2016, **4**(23), 8932–8951.
6 R. C. Haddon, Carbon nanotubes, *Acc. Chem. Res.*, 2002, **35**(12), 997.
7 C. Liu and H. M. Cheng, Controlled Growth of Semiconducting and Metallic Single-Wall Carbon Nanotubes, *J. Am. Chem. Soc.*, 2016, **138**(21), 6690–6698.
8 H. Amara and C. Bichara, Modeling the Growth of Single-Wall Carbon Nanotubes, *Top. Curr. Chem.*, 2017, **375**(3), 55.
9 J. Huang, Q. Zhang, M. Zhao and F. Wei, A review of the large-scale production of carbon nanotubes: The practice of nanoscale process engineering, *Chin. Sci. Bull.*, 2012, **57**(2), 157–166.
10 H. Wang, C. Yamada, J. Liu, B. Liu, X. Tu, M. Zheng, *et al.*, Re-growth of single-walled carbon nanotube by hot-wall and cold-wall chemical vapor deposition, *Carbon*, 2015, **95**, 497–502.
11 G. P. Gakis, S. Termine, A.-F. A. Trompeta, I. G. Aviziotis and C. A. Charitidis, Unraveling the mechanisms of carbon nanotube growth by chemical vapor deposition, *Chem. Eng. J.*, 2022, **445**, 136807.
12 X. Jia and F. Wei, Advances in Production and Applications of Carbon Nanotubes, *Top. Curr. Chem.*, 2017, **375**(1), 18.
13 X. Zhu, X. Wu, T. N. L. Doan, Y. Tian, H. Zhao and P. Chen, Binder-free flexible $LiMn_2O_4$/carbon nanotube network as high power cathode for rechargeable hybrid aqueous battery, *J. Power Sources*, 2016, **326**, 498–504.
14 X. Zhu, S. H. Choi, R. Tao, X. Jia and Y. Lu, Building high-rate silicon anodes based on hierarchical Si@C@CNT nanocomposite, *J. Alloys Compd.*, 2019, **791**, 1105–1113.
15 A. J. Clancy, J. Melbourne and M. S. P. Shaffer, A one-step route to solubilised, purified or functionalised single-walled carbon nanotubes, *J. Mater. Chem. A*, 2015, **3**(32), 16708–16715.
16 F. Lou, H. Zhou, T. D. Tran, M. E. Melandsø Buan, F. Vullum-Bruer, M. Rønning, *et al.*, Coaxial Carbon/Metal Oxide/Aligned Carbon Nanotube Arrays as High-Performance Anodes for Lithium Ion Batteries, *ChemSusChem*, 2014, **7**(5), 1201.

17 Y. Luo, K. Wang, Q. Li, S. Fan and J. Wang, Macroscopic Carbon Nanotube Structures for Lithium Batteries, *Small*, 2020, **16**(15), 1902719.
18 S. Zhu and J. Ni, The Critical Role of Carbon Nanotubes in Bridging Academic Research to Commercialization of Lithium Batteries, *Chem. Rec.*, 2022, **22**(10), e202200125.
19 S. Xie, W. Li, Z. Pan, B. Chang and L. Sun, Carbon nanotube arrays, *J. Mater. Sci. Eng. A*, 2000, **286**(1), 11–15.
20 I. A. Kinloch, J. Suhr, J. Lou, R. J. Young and P. M. Ajayan, Composites with carbon nanotubes and graphene: an outlook, *Science*, 2018, **362**(6414), 547–553.
21 J. Vejpravova, B. Pacakova and M. Kalbac, Magnetic impurities in single-walled carbon nanotubes and graphene: a review, *Analyst*, 2016, **141**(9), 2639–2656.
22 Q. Zhang, J.-Q. Huang, M.-Q. Zhao, W.-Z. Qian and F. Wei, Carbon Nanotube Mass Production: Principles and Processes, *ChemSusChem*, 2011, **4**(7), 864–889.
23 J. L. Zimmerman, R. K. Bradley, C. B. Huffman, R. H. Hauge and J. L. Margrave, Gas-Phase Purification of Single-Wall Carbon Nanotubes, *Chem. Mater.*, 2000, **12**(5), 1361–1366.
24 I. W. Chiang, B. E. Brinson, R. E. Smalley, J. L. Margrave and R. H. Hauge, Purification and Characterization of Single-Wall Carbon Nanotubes, *J. Phys. Chem. B*, 2001, **105**(6), 1157–1161.
25 T.-C. Chen, M.-Q. Zhao, Q. Zhang, G.-L. Tian, J.-Q. Huang and F. Wei, *In Situ* Monitoring the Role of Working Metal Catalyst Nanoparticles for Ultrahigh Purity Single-Walled Carbon Nanotubes, *Adv. Funct. Mater.*, 2013, **23**(40), 5066–5073.
26 B. P. Bittova, M. Kalbac, S. Kubickova, A. Mantlikova, S. Mangold and J. Vejpravova, Structure and magnetic response of a residual metal catalyst in highly purified single walled carbon nanotubes, *Phys. Chem. Chem. Phys.*, 2013, **15**(16), 5992–6000.
27 A. C. Dillon, T. Gennett, K. M. Jones, J. L. Alleman, P. A. Parilla and M. J. Heben, A Simple and Complete Purification of Single-Walled Carbon Nanotube Materials, *Adv. Mater.*, 1999, **11**(16), 1354–1358.
28 A. Aghaei, M. Shaterian, H. Hosseini-Monfared and A. Farokhi, Single-walled carbon nanotubes: synthesis and quantitative purification evaluation by acid/base treatment for high carbon impurity elimination, *Chem. Pap.*, 2023, **77**(1), 249–258.
29 E. R. Edwards, E. F. Antunes, E. C. Botelho, M. R. Baldan and E. J. Corat, Evaluation of residual iron in carbon nanotubes purified by acid treatments, *Appl. Surf. Sci.*, 2011, **258**(2), 641–648.
30 Y. Liu, Y. Wang, Y. Liu, W. Li, W. Zhou and F. Wei, Purifying double-walled carbon nanotubes by vacuum high-temperature treatment, *Nanotechnology*, 2007, **18**(17), 175704.
31 A. Desforges, A. V. Bridi, J. Kadok, E. Flahaut, F. Le Normand, J. Gleize, *et al.*, Dramatic enhancement of double-walled carbon nanotube quality through a one-pot tunable purification method, *Carbon*, 2016, **110**, 292–303.
32 S. H. Wang, R. H. Hauge, M. Pasquali and R. E. Smalley, A Highly Selective, One-Pot Purification Method for Single-Walled Carbon Nanotubes, *J. Phys. Chem. B*, 2007, **111**(6), 1249–1252.
33 A. Suri and K. S. Coleman, The superiority of air oxidation over liquid-phase oxidative treatment in the purification of carbon nanotubes, *Carbon*, 2011, **49**(9), 3031–3038.
34 A. J. Clancy, E. R. White, H. H. Tay, H. C. Yau and M. S. P. Shaffer, Systematic comparison of conventional and reductive single-walled carbon nanotube purifications, *Carbon*, 2016, **108**, 423–432.
35 H. Hu, B. Zhao, M. E. Itkis and R. C. Haddon, Nitric Acid Purification of Single-Walled Carbon Nanotubes, *J. Phys. Chem. B*, 2003, **107**(50), 13838–13842.
36 P. X. Hou, S. Bai, Q. H. Yang, C. Liu and H. M. Cheng, Multi-step purification of carbon nanotubes, *Carbon*, 2002, **40**(1), 81–85.
37 S. Yasuda, T. Hiraoka, D. N. Futaba, T. Yamada, M. Yumura and K. Hata, Existence and Kinetics of Graphitic Carbonaceous Impurities in Carbon Nanotube Forests to Assess the Absolute Purity, *Nano Lett.*, 2009, **9**(2), 769–773.
38 A. D. Jara, A. Betemariam, G. Woldetinsae and J. Y. Kim, Purification, application and current market trend of natural graphite: a review, *Int. J. Min. Sci. Technol.*, 2019, **29**(5), 671–689.
39 W. Huang, Y. Wang, G. Luo and F. Wei, 99.9% purity multi-walled carbon nanotubes by vacuum high-temperature annealing, *Carbon*, 2003, **41**(13), 2585–2590.
40 M. Yudasaka, T. Ichihashi, D. Kasuya, H. Kataura and S. Iijima, Structure changes of single-wall carbon nanotubes and single-wall carbon nanohorns caused by heat treatment, *Carbon*, 2003, **41**(6), 1273–1280.
41 NIST-JANAF, (n.d.). **https://janaf.nist.gov/tables/Cl-index.html** (accessed October 31, 2023).
42 G. Mercier, C. Hérold, J.-F. Marêché, S. Cahen, J. Gleize, J. Ghanbaja, *et al.*, Selective removal of metal impurities from single walled carbon nanotube samples, *New J. Chem.*, 2013, **37**(3), 790–795.
43 H. Tanaka, T. Goto, K. Hamada, K. Ohashi, T. Osawa, H. Sugime, *et al.*, Safe and damage-less dry-purification of carbon nanotubes using $FeCl_3$ vapor, *Carbon*, 2023, **212**, 118171.